**FACTA UNIVERSITATIS**
Series: **Physics, Chemistry and Technology** Vol. 17, N° 2, 2019, pp. 173 - 190
https://doi.org/10.2298/FUPCT1902173F

# SLOW AND FAST LIGHT PROPAGATION THROUGH LADDER-TYPE ATOMIC MEDIA WITH DEGENERATE ENERGY LEVELS†

*UDC 535.353*

**Nikola Filipović, Vladan Pavlović, Ljiljana Stevanović**

Department of Physics, Faculty of Sciences and Mathematics, University of Niš, Serbia

**Abstract**. *We investigate the weak probe pulse propagation through the atomic medium, in the presence of the strong control laser field, under the regime of the electromagnetically induced transparency (EIT). These fields couple to the medium by forming the 3-level ladder configuration. We focus on two distinct cases: closed system, which is a non-degenerate, and open system, where the middle level is 3-fold degenerate, and the additional levels are coupled to the other levels only via spontaneous emission. The spatio-temporal profile of the probe pulse envelope is obtained by using the formalism of Maxwell-Bloch equations with the help of the Fourier transform method. We study the influence of the control field Rabi frequency, the spectral half-width of the initial pulse and decay rates on the propagation of the probe pulse. Several important pulse parameters are also calculated and discussed. It is shown that the group velocity of light can be controlled in such a manner that one can switch from slow to fast light and vice versa when changing the control Rabi frequency and spectral pulse half-width. Moreover, the possibility of replacing the open with an effective closed system is also discussed.*

**Key words**: *Electromagnetically induced transparency, Slow light, Fast light, Energy level degeneracy, Closed system, Open system*

## 1. INTRODUCTION

During the past years, the substantial progress has been made in the field of the laser pulse propagation through various gaseous and cold-atomic media, even in the cases when the probe light intensity is very low (few photons per cross-section, Menzel, 2007, Scully and Zubairy, 1997). This is enabled by taking advantage of the quantum interference effect called electromagnetically induced transparency (EIT), which requires

Received Match 26th, 2019; accepted December 24th, 2019
† Acknowledgements**:** This paper is the part of the research supported by projects III45010, OI171028 and OI171025 of the Ministry of Education, Science and Technological Development of Republic of Serbia.
**Corresponding author:** Nikola Filipović, Department of Physics, Faculty of Sciences and Mathematics, University of Niš, Višegradska 33, 18000 Niš • E-mail: nikola.filipovic@pmf.edu.rs

the presence of one or more strong control fields (Fleischhauer et al., 2005, Marangos, 1998). Under EIT conditions, the medium, previously opaque for probe light at the specific (resonant) frequency, now becomes transparent. The first experimental demonstration of the EIT was done by Boller et. al. in 1990 on strontium vapors (Boller et al., 1991). Under the EIT regime, the dispersion properties of the atomic medium are changed, thus leading to the formation of slow light which propagates through the medium with very small group velocity, which is experimentally achieved on lead vapors in 1992 by Harris et. al, with the group velocity of light being reduced 250 times (Harris et al., 1992). By using such media, it became possible to reduce the group velocity of light to 90 m/s in the optically dense hot rubidium gas (Kash et al., 1999), 17 m/s in the ultracold gas of sodium atoms (Hau et al., 1999), and even to 8 m/s in rubidium vapors (Budker et al., 1999). Furthermore, the complete light storage and pulse revival is performed by switching the control field(s) off, and then back on. With this technique, the original pulse can almost completely be recovered, which means that EIT media can serve as quantum memory elements based on the light storage (Lukin, 2003, Zhang et al., 2011). By changing the properties of the control field(s) and other parameters, and thus affecting the occurrence of the EIT window, one can switch between slow light and fast light, which is the regime where the group velocity of light is larger than the vacuum speed of light (Boyd and Gauthier, 2009, Boyd and Narum, 2007). This property of such atom-lasers systems can be of use in the construction of optical switches and other optical devices, as well as in various applications in the fields of quantum optics and quantum information processing (Schmidt and Ram, 2000, Vitali et al., 2000).

In many atom-lasers systems where the EIT effect is studied, one usually considers the set of energy levels where all the levels are coupled to one or several other levels from the same set via laser fields (closed quantum systems). This approach, however, does not allow much flexibility in the choice of the atom-lasers system which can be studied. The reason is that there are many systems of interest with one or several energy levels that are not coupled to any of the laser fields, but affect the whole system via spontaneous emission from and to other energy levels (open quantum systems). For instance, the experiments concerning the EIT are typically realized using atoms of alkaline (Rb, Na), alkaline earth (Sr, Ca) and rare earth metals (Yb). According to this, the levels of interest are their specific hyperfine levels. For example, when studying the lambda-type EIT, one can isolate the D1 levels of the $^{87}$Rb – namely, $5S_{1/2}, F = 1$, $5S_{1/2}, F = 2$ and $5P_{1/2}, F = 1$. Here, one must consider the Zeeman degeneracy of these levels, which causes the system to be considered as the “chain lambda-type system”, i.e. the effective lambda-type system (Li et al., 2011, Li and Xiao, 1995). On the other hand, for the ladder-type EIT, the following levels of interest are chosen: $5S_{1/2}, F = 1$, $5P_{3/2}, F = 2$ and $5D_{5/2}, F = 3$. The existence of the Zeeman degeneracy, in this case, leads to the fact that the spontaneous decay of the middle level $5P_{3/2}, F = 2$) causes the increase of the population of the second hyperfine level of the ground state ($5S_{1/2}, F = 2$). This effect can create the optical pumping phenomenon, which can cover up the EIT spectrum if the real system is considered as the simple, closed three-level ladder-type system (Noh and Moon, 2009, Noh and Moon, 2012). Therefore, one has to deal with the level of degeneracy by modeling its existence and physical implications by the effective 3-level system (Badger et al., 2001, Guan and Yu, 2000, Moon and Noh, 2013, Reshetov and Meleshko, 2014). Some part of the research is already conducted in our previous work, where the detailed examination of the absorption and dispersion curve with respect to several important parameters is given (Stevanović et al., 2018). We expand this vital study by focusing on the propagation of light through the EIT medium and investigating how the energy level degeneracy affects the probe pulse and parameters relevant to it, such as the group index, pulse duration and transmission coefficient.

The degeneracy of the energy levels is not the exclusive property of gaseous media. The significant attention has been given to the study of the propagation of light through the solid-state media as well. Moreover, the discrete energy structure similar to one of the atoms is achieved in semiconductor heterostructures, such as quantum dots, which is why they are usually called artificial atoms. Here, the degeneracy of certain levels is also an important research topic. For instance, our previous research dealt with the EIT effect on the energy levels of the hydrogen impurity located in the center of the semiconductor spherical quantum dot (Pavlović and Stevanović, 2016, Pavlović et al., 2018). This study focuses on the interaction of the laser fields with the confined hydrogen atom, modeled as the three- or four-level system in the ladder configuration. Here, the polarization of the laser fields is chosen in such a way that they couple to the particular energy levels of the configuration and no other levels are considered, thus forming the closed system. For example, in Pavlović et al., 2018, the laser polarization is such that the probe laser excites the transition $1s_0 \rightarrow 2p_{-1}$, while the control laser excites the transition $2p_{-1} \rightarrow 3d_{-2}$. As determined by the selection rules, level $2p_{-1}$ decays to the level $1s_0$ only, while level $3d_{-2}$ undergoes the spontaneous emission exclusively to the level $2p_{-1}$. However, if the polarization of the laser is chosen in a different way, such that the probe laser excites the transition $1s_0 \rightarrow 2p_{-1}$, while the control laser excites the transition $2p_{-1} \rightarrow 3d_0$, the highest level $3d_0$ then decays to the levels $2p_{-1}$, $2p_0$ and $2p_{+1}$, which, due to the spherical symmetry of the problem, all have the same energy. Therefore, this paper should explain how the existence of the additional levels $2p_0$ and $2p_{+1}$ affects the parameters responsible for the appearance of the EIT effect, as well as the shape of the probe pulse itself at the exit of the medium. When dealing with these systems, one has to keep in mind the main difference between solid-state and gaseous systems – for solid-state systems, in addition to the spontaneous emission, decoherence processes due to the electron-phonon interaction are also present and cannot be omitted even on room temperatures. Since we assume that only the decay processes due to the spontaneous emission are present in the systems we explore in this paper, we dedicate our research to the gaseous atomic systems and solid-state systems on cryogenic temperatures, where the spontaneous emission is the dominant source of decoherence.

In this paper, the propagation of the weak probe laser pulse through the atomic medium in the presence of the additional, strong control field is studied. This atom-lasers system forms the 3-level ladder coupling scheme and satisfies the EIT condition in most of the paper. We distinguish between two cases: the first, where the atomic system is non-degenerate, and all the levels from the chosen set of energy levels are coupled to the corresponding levels of the same set via electromagnetic fields forming the closed quantum system, and the second, where the middle level is 3-fold degenerate, and the additional energy levels (two sublevels of the middle level) are not coupled to other levels via electromagnetic fields, but only through the spontaneous emission. In addition, we concentrate on the case where all the decoherence is completely due to the spontaneous emission, which practically holds for all the gaseous media used in EIT experiments, as well as for the solid-state media at cryogenic temperatures. In order to compute the spatio-temporal profile of the envelope of the probe pulse, we adopt the density matrix formalism and solve Maxwell-Bloch equations with the help of the Fourier transform method. The obtained results are then analyzed with respect to the control field Rabi frequency, the spectral half-width of the input pulse and decay rates. Moreover, on the basis of these results, the group index, relative temporal pulse width and transmission coefficient are also calculated and discussed. We also discuss the differences between the probe pulse propagation for the closed and open system, as well as the possibility of replacing the open system with the closed system with the effective decay rate.

This paper is organized as follows. In Section 2, we give the theoretical overview of the system in question, as well as the derivation of Maxwell-Bloch equations for the closed and open system. The solution process of Maxwell-Bloch equations is presented in Section 3, while in Section 4 the detailed analysis of the obtained results is given. Finally, we end this paper with a brief conclusion.

## 2. Theoretical Background

We study the interaction of two electromagnetic fields with a certain atomic medium. Since our method is general, we do not specify the type of the medium – it can usually be an atomic gas, but the same formalism can be used for solid-state systems, such as artificial atoms. For the sake of simplicity, we use the term "atomic medium" when we refer to the quantum system with which laser fields interact. In this paper, we assume that the two laser fields, the weak probe field $\vec{\mathcal{E}}_p$ and strong control field $\vec{\mathcal{E}}_c$, are coupled to the atomic medium by forming the ladder coupling scheme (Fig. 1). In Fig. 1 (a), all the levels of the chosen system are coupled to the corresponding levels of the same system via electromagnetic fields, and such a system is therefore called the *closed* quantum system. The energy levels of this system are labeled with $|1\rangle$, $|2\rangle$, and $|3\rangle$, with the corresponding energy values $E_1$, $E_2$ and $E_3$. Here, the dipole-allowed transitions are $|1\rangle \leftrightarrow |2\rangle$ (coupled by the probe field) and $|2\rangle \leftrightarrow |3\rangle$ (coupled by the control field), while $|1\rangle \leftrightarrow |3\rangle$ is a dipole-forbidden transition. On the other hand, we are also interested in the case when the middle level $|2\rangle$ is 3-fold degenerate, which is often the case for hyperfine levels of the alkaline atoms, which are usually used as a medium in EIT experiments. (Badger et al., 2001, Guan and Yu, 2000, Li and Xiao, 1995, Moon and Noh, 2013, Noh and Moon, 2009, Noh and Moon, 2012). Therefore, the other system of interest is depicted on Fig. 1 (b), obeying the same selection rules as the closed system and containing the two additional levels $|4\rangle$ and $|5\rangle$, with the energies $E_4 = E_5 = E_2$. These two levels are not coupled to the laser fields but participate in decay processes, which is why this system is called the *open* quantum system (Moon and Noh, 2013).

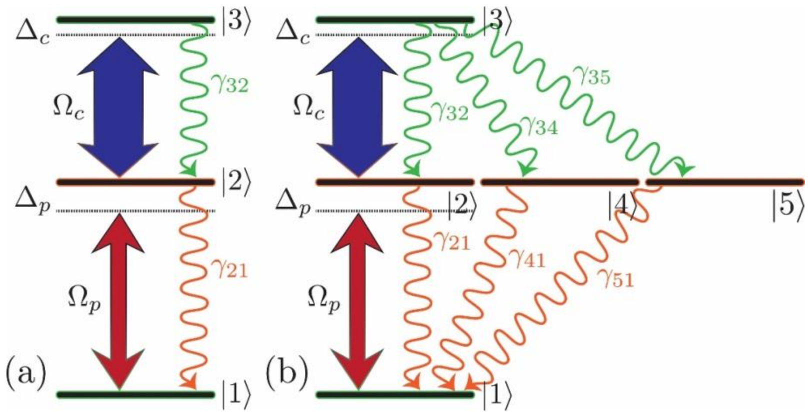


**Fig. 1** The ladder atom-lasers coupling scheme for the (a) closed and (b) open quantum system. All the relevant quantities are labeled and explained in the main text.

In both cases, the Hamiltonian of the whole atom-lasers system is $H = H_0 + V$, where $H_0$ is the free atom Hamiltonian ($H_0|i\rangle = E_i|i\rangle$, with $E_i$ being the energy of the eigenstate $|i\rangle$ of the atom) and $V = -\mathbf{d} \cdot (\vec{\mathcal{E}}_p + \vec{\mathcal{E}}_c)$ is the interaction term, with $\mathbf{d}$ being the electric dipole operator. The electric field strengths of the probe and control laser are given by the following expressions:

$$\vec{\mathcal{E}}_p = \frac{1}{2}\left(\mathbf{E}_p e^{-i\omega_p t} + \mathbf{E}_p^* e^{i\omega_p t}\right),\ \vec{\mathcal{E}}_c = \frac{1}{2}\left(\mathbf{E}_c e^{-i\omega_c t} + \mathbf{E}_c^* e^{i\omega_c t}\right), \quad (1)$$

where $\mathbf{E}_p$ ($\mathbf{E}_c$) and $\omega_p$ ($\omega_c$) stand for the complex electric field envelope and frequency of the probe (control) field, respectively. Having this in mind, and using the dipole and rotating-wave approximation in the co-rotating frame, the system Hamiltonian is reduced to the form (Stevanović et al., 2018):

$$H = -\hbar\Omega_p^* S_{12} - \hbar\Omega_p S_{21} + \hbar\Delta_p S_{22} - \hbar\Omega_c^* S_{23} - \hbar\Omega_c S_{32} + \hbar\left(\Delta_p + \Delta_c\right)S_{33}, \quad (2)$$

where $S_{ij} = |i\rangle\langle j|$, which is the same for both the closed and open system. In the former expression, $\Omega_p = \mathbf{d}_{21} \cdot \mathbf{E}_p/(2\hbar)$ ($\Omega_c = \mathbf{d}_{32} \cdot \mathbf{E}_c/(2\hbar)$) and $\Delta_p = \omega_{21} - \omega_p$ ($\Delta_c = \omega_{32} - \omega_c$) represent the Rabi frequency and the detuning of the probe (control) laser field, with $\mathbf{d}_{21}$ ($\mathbf{d}_{32}$) and $\omega_{21} = (E_2 - E_1)/\hbar$ ($\omega_{32} = (E_3 - E_2)/\hbar$) being the electric dipole transition matrix element and transition frequency for the transition $|1\rangle \leftrightarrow |2\rangle$ ($|2\rangle \leftrightarrow |3\rangle$), respectively.

In order to investigate the probe pulse propagation through the atomic medium, the density matrix formalism is firstly adopted. By knowing the Hamiltonian of the system of interest, the dynamics of the density matrix operator $\rho$ can be determined by the Liouville equation (Scully and Zubairy, 1997):

$$\frac{d\rho}{dt} = -\frac{i}{\hbar}[H, \rho] + \Lambda\rho, \quad (3)$$

where the term $\Lambda\rho$ describes decoherence effects, which origin can generally be very different. Here, we shall assume that the dominant source of decoherence is the spontaneous emission, which is justified for atomic gases and for solid-state media at cryogenic temperatures when the electron-phonon interaction is negligible. According to this, the decoherence term yields

$$\Lambda\rho = -\frac{1}{2}\gamma_{21}(\rho S_{22} + S_{22}\rho - 2\rho_{22}S_{11}) - \frac{1}{2}\gamma_{41}(\rho S_{44} + S_{44}\rho - 2\rho_{44}S_{11}) - \frac{1}{2}\gamma_{51}(\rho S_{55} + S_{55}\rho - 2\rho_{55}S_{11}) - \frac{1}{2}\gamma_{32}(\rho S_{33} + S_{33}\rho - 2\rho_{33}S_{22}) - \frac{1}{2}\gamma_{34}(\rho S_{33} + S_{33}\rho - 2\rho_{33}S_{44}) - \frac{1}{2}\gamma_{35}(\rho S_{33} + S_{33}\rho - 2\rho_{33}S_{55}), \quad (4)$$

where the decay rate from state $|i\rangle$ to $|j\rangle$ due to the spontaneous emission is given by the well-known formula:

$$\gamma_{ij} = \frac{\omega_{ij}^3 |\mathrm{d}_{ij}|^2}{6\pi\varepsilon_0\hbar c^3}. \quad (5)$$

Eq. 4 is written for the open system, and the corresponding expression for the closed system can be obtained if we set $\gamma_{34} = \gamma_{35} = \gamma_{41} = \gamma_{51} = 0$.

By replacing Eqs. 2 and 4 into Eq. 3, we obtain the optical Bloch equations (OBEs) for both the closed and open systems. For the closed system, we have

$$\dot{\rho}_{11} = i(\Omega_p^*\rho_{21} - \Omega_p\rho_{12}) + \gamma_{21}\rho_{22}, \quad (6)$$

$$\dot{\rho}_{21} = i\left(\Omega_c\rho_{31} - \Delta_p\rho_{21} + \Omega_p(\rho_{11} - \rho_{22})\right) - \frac{1}{2}\gamma_{21}\rho_{21}, \quad (7)$$

$$\dot{\rho}_{31} = i(\Omega_c\rho_{21} - (\Delta_p + \Delta_c)\rho_{31} - \Omega_p\rho_{32}) - \frac{1}{2}\gamma_{32}\rho_{31}, \quad (8)$$

$$\dot{\rho}_{32} = i(\Omega_c(\rho_{22} - \rho_{33}) - \Delta_c\rho_{32} - \Omega_p^*\rho_{31}) - \frac{1}{2}(\gamma_{21} + \gamma_{32})\rho_{32}, \quad (9)$$

$$\dot{\rho}_{33} = i(\Omega_c\rho_{23} - \Omega_c^*\rho_{32}) - \gamma_{32}\rho_{33}, \quad (10)$$

$$1 = \rho_{11} + \rho_{22} + \rho_{33}, \quad (11)$$

while the OBEs for the open quantum system have the following form:

$$\dot{\rho}_{11} = i(\Omega_p^*\rho_{21} - \Omega_p\rho_{12}) + \gamma_{21}\rho_{22} + \gamma_{41}\rho_{44} + \gamma_{51}\rho_{55}, \quad (12)$$

$$\dot{\rho}_{21} = i(\Omega_c^*\rho_{31} - \Delta_p\rho_{21} + \Omega_p(\rho_{11} - \rho_{22})) - \frac{1}{2}\gamma_{21}\rho_{21}, \quad (13)$$

$$\dot{\rho}_{31} = i(\Omega_c\rho_{21} - (\Delta_p + \Delta_c)\rho_{31} - \Omega_p\rho_{32}) - \frac{1}{2}(\gamma_{32} + \gamma_{34} + \gamma_{35})\rho_{31}, \quad (14)$$

$$\dot{\rho}_{41} = -i\Omega_p\rho_{42} - \frac{1}{2}\gamma_{41}\rho_{41}, \quad (15)$$

$$\dot{\rho}_{51} = -i\Omega_p\rho_{52} - \frac{1}{2}\gamma_{51}\rho_{51}, \quad (16)$$

$$\dot{\rho}_{32} = i(\Omega_c(\rho_{22} - \rho_{33}) - \Delta_c\rho_{32} - \Omega_p^*\rho_{31}) - \frac{1}{2}(\gamma_{21} + \gamma_{32} + \gamma_{34} + \gamma_{35})\rho_{32}, \quad (17)$$

$$\dot{\rho}_{42} = i(\Delta_p\rho_{42} - \Omega_p^*\rho_{41} - \Omega_c\rho_{43}) - \frac{1}{2}(\gamma_{21} + \gamma_{41})\rho_{42}, \quad (18)$$

$$\dot{\rho}_{52} = i(\Delta_p\rho_{52} - \Omega_p^*\rho_{51} - \Omega_c\rho_{53}) - \frac{1}{2}(\gamma_{21} + \gamma_{51})\rho_{52}, \quad (19)$$

$$\dot{\rho}_{33} = i(\Omega_c\rho_{23} - \Omega_c^*\rho_{32}) - (\gamma_{32} + \gamma_{34} + \gamma_{35})\rho_{33}, \quad (20)$$

$$\dot{\rho}_{43} = i\left(\left(\Delta_p + \Delta_c\right)\rho_{43} - \Omega_c^*\rho_{42}\right) - \frac{1}{2}(\gamma_{41} + \gamma_{32} + \gamma_{34} + \gamma_{35})\rho_{43}, \tag{21}$$

$$\dot{\rho}_{53} = i\left(\left(\Delta_p + \Delta_c\right)\rho_{53} - \Omega_c^*\rho_{52}\right) - \frac{1}{2}(\gamma_{51} + \gamma_{32} + \gamma_{34} + \gamma_{35})\rho_{53}, \tag{22}$$

$$\dot{\rho}_{44} = -\gamma_{41}\rho_{44} + \gamma_{34}\rho_{33}, \tag{23}$$

$$\dot{\rho}_{54} = -\frac{1}{2}(\gamma_{41} + \gamma_{51})\rho_{54}, \tag{24}$$

$$\dot{\rho}_{55} = -\gamma_{51}\rho_{55} + \gamma_{35}\rho_{33}, \tag{25}$$

$$1 = \rho_{11} + \rho_{22} + \rho_{33} + \rho_{44} + \rho_{55}, \tag{26}$$

where $\rho_{ij}^* = \rho_{ji}$ and Eqs. 11 and 26 represent the closure relations for the closed and open system, respectively.

We complete the system of equations by adding the propagation equation for the probe field. In our case, we assume that the probe laser is a pulsed laser (with a temporal profile) which spreads all over the medium, and the control laser, which also covers the whole atomic sample, is a continuous-wave (cw) laser and no propagation equation for the control field is necessary. We choose the $z$-axis to be the propagation axis, so $\mathbf{E}_p = \mathbf{E}_p(z,t)$ and consequently $\Omega_p = \Omega_p(z,t)$, while $\Omega_c = \text{const.}$, and both the probe and control field being polarized in the transverse direction with the unit vector $\hat{\mathbf{n}}$. If the described coordinate system is chosen, we can rewrite the probe and control Rabi frequency as $\Omega_p = d_{21}E_p/(2\hbar)$ and $\Omega_c = d_{32}E_p/(2\hbar)$, respectively, where $E_p$ ($E_c$) is the absolute value of the probe (control) electric field envelope, $d_{ij} = -\,e\langle i|\mathbf{r}\cdot\hat{\mathbf{n}}|j\rangle$, $\mathbf{r}$ is the radius vector and $e$ is the electron charge. The probe field propagation equation is then obtained from the wave equation, after the slowly-varying envelope approximation has been made, and takes the form (Boyd, 2007):

$$\left(\frac{\partial}{\partial z} + \frac{1}{c}\frac{\partial}{\partial t}\right)E_p = i\frac{\omega_p}{2\varepsilon_0 c}P_p. \tag{27}$$

Here, $P_p$ is the envelope of the electric polarization of the medium due to the existence of the probe field, and can be calculated by knowing the coherence $\rho_{21}$, which corresponds to the transition $|1\rangle \leftrightarrow |2\rangle$:

$$P_p = N\langle d_{21}\rangle = N\,\mathrm{Tr}(\rho d) = Nd_{21}\rho_{21}, \tag{28}$$

where $N$ is the density of atoms inside the medium. By substituting Eq. 28 into Eq. 27, the propagation equation yields

$$\left(\frac{\partial}{\partial z} + \frac{1}{c}\frac{\partial}{\partial t}\right)E_p = i\frac{N\omega_p d_{21}}{2\varepsilon_0 c}\rho_{21}. \tag{29}$$

Eq. 29, together with Eqs. 6–11 (12–26) forms the Maxwell-Bloch equations for the closed (open) quantum system.

## 3. THE SOLUTION OF MAXWELL-BLOCH EQUATIONS

In the EIT regime, $\Omega_p \ll \Omega_c$ and it is reasonable to adopt the perturbation method to solve Maxwell-Bloch equations. More precisely, one can treat the probe Rabi frequency as a perturbation and make a replacement $\Omega_p \to \lambda\Omega_p$, where $\lambda$ is a small parameter. In addition, density matrix elements can be expanded as $\rho_{ij} = \sum_{n=0}^{\infty} \lambda^n \rho_{ij}^{(n)}$, and only the first-order terms (linear in $\Omega_p$) can be retained. After this linearization procedure, one can find that the only relevant equations from the system of Eqs. 6–11 are

$$\dot{\rho}_{21} = i\Omega_p + i\Omega_c^* \rho_{31} - \left(i\Delta_p + \frac{1}{2}\gamma_{21}\right)\rho_{21}, \tag{30}$$

$$\dot{\rho}_{31} = i\Omega_c \rho_{21} - \left(i\left(\Delta_p + \Delta_c\right) + \frac{1}{2}\gamma_{32}\right)\rho_{31}, \tag{31}$$

for the closed system, while the system of Eqs. 12–26 reduces to

$$\dot{\rho}_{21} = i\Omega_p + i\Omega_c^* \rho_{31} - \left(i\Delta_p + \frac{1}{2}\gamma_{21}\right)\rho_{21}, \tag{32}$$

$$\dot{\rho}_{31} = i\Omega_c \rho_{21} - \left(i\left(\Delta_p + \Delta_c\right) + \frac{1}{2}(\gamma_{32} + \gamma_{34} + \gamma_{35})\right)\rho_{31}, \tag{33}$$

for the open system, where we wrote $\rho_{ij} = \rho_{ij}^{(1)}$ in order to simplify the notation. Moreover, we assume that the whole atomic system is initially prepared in the ground state $|1\rangle$, thus $\rho_{11}^{(0)} = 1$ and $\rho_{ij}^{(0)} = 0,\ ij \neq 11$. Note that the Eqs. 30 and 32 have the same form, and that the decay rates $\gamma_{41}$ and $\gamma_{51}$ do not enter the relevant OBEs for the open system, and therefore do not affect the behavior of the open system in the first order in $\Omega_p$. However, in the situations where the EIT condition is no longer satisfied, the use of the perturbation approach is no longer legitimate, and the higher orders in $\Omega_p$ need to be taken into account. In such cases, decay rates $\gamma_{41}$ and $\gamma_{51}$ enter OBEs regularly.

Since the density matrix elements (together with the probe Rabi frequency) are time-dependent quantities (they depend on the $z$-coordinate as well), the Fourier transform method is used in order to eliminate time derivatives from OBEs and obtain the system of algebraic equations which drastically simplifies the solution process. If we take the Fourier transform of both the Eqs. 30 and 31 with respect to time, we have

$$-i\omega\tilde{\rho}_{21} = i\tilde{\Omega}_p + i\Omega_c^* \tilde{\rho}_{31} - \left(i\Delta_p + \frac{1}{2}\gamma_{21}\right)\tilde{\rho}_{21}, \tag{34}$$

$$-i\omega\tilde{\rho}_{31} = i\Omega_c \tilde{\rho}_{21} - \left(i\left(\Delta_p + \Delta_c\right) + \frac{1}{2}\gamma_{32}\right)\tilde{\rho}_{31}, \tag{35}$$

for the closed system, where $\omega$ stands for the frequency of the particular Fourier component of the probe pulse, and $\tilde{\rho}_{21}(z,\omega)$, $\tilde{\rho}_{31}(z,\omega)$ and $\tilde{\Omega}_p(z,\omega)$ represent the Fourier transforms of $\rho_{21}(z,t)$, $\rho_{31}(z,t)$ and $\Omega_p(z,t)$, respectively. Similarly, by taking the Fourier transform of Eqs. 32 and 33, we obtain

$$-i\omega\tilde{\rho}_{21} = i\tilde{\Omega}_p + i\Omega_c^* \tilde{\rho}_{31} - \left(i\Delta_p + \frac{1}{2}\gamma_{21}\right)\tilde{\rho}_{21}, \tag{36}$$

$$-i\omega\tilde{\rho}_{31} = i\Omega_c \tilde{\rho}_{21} - \left(i\left(\Delta_p + \Delta_c\right) + \frac{1}{2}(\gamma_{32} + \gamma_{34} + \gamma_{35})\right)\tilde{\rho}_{31}, \tag{37}$$

which hold for the open system. After eliminating $\tilde{\rho}_{31}$ from both of the two systems of equations, we obtain the same expression:

$$\tilde{\rho}_{21} = f(\omega)\widetilde{\Omega}_p = f(\omega)\frac{d_{21}}{2\hbar}\tilde{E}_p, \tag{38}$$

for both the closed and open quantum systems. The difference, however, lies in the expression for the function $f(\omega)$, which, for the closed system, yields

$$f_{\text{closed}}(\omega) = \frac{\omega-\Delta_p-\Delta_c+\frac{1}{2}i\gamma_{32}}{|\Omega_c|^2-\left(\omega-\Delta_p+\frac{1}{2}i\gamma_{21}\right)\left(\omega-\Delta_p-\Delta_c+\frac{1}{2}i\gamma_{32}\right)}, \tag{39}$$

while, for the open system, we have

$$f_{\text{open}}(\omega) = \frac{\omega-\Delta_p-\Delta_c+\frac{1}{2}i(\gamma_{32}+\gamma_{34}+\gamma_{35})}{|\Omega_c|^2-\left(\omega-\Delta_p+\frac{1}{2}i\gamma_{21}\right)\left(\omega-\Delta_p-\Delta_c+\frac{1}{2}i(\gamma_{32}+\gamma_{34}+\gamma_{35})\right)}. \tag{40}$$

This function is, in both cases, connected to the electric susceptibility with respect to the probe field, and thus to the polarization to the probe field, which enters the propagation equation, Eq. 29. We note that the main difference between $f_{\text{closed}}(\omega)$ and $f_{\text{open}}(\omega)$ can be seen by looking at the terms which contain decay rates – for the open system, there are additional decay processes due to the existence of the levels $|4\rangle$ and $|5\rangle$.

In order to utilize the previously obtained expressions, one has to take the Fourier transform of Eq. 29 as well. Consequently, the equation for the Fourier amplitude of the probe field envelope $\tilde{E}_p(z,\omega)$ now yields

$$\left(\frac{\partial}{\partial z} - i\kappa(\omega)\right)\tilde{E}_p(z,\omega) = 0, \tag{41}$$

where

$$\kappa(\omega) = \frac{\omega}{c} + \alpha f(\omega), \tag{42}$$

and $\alpha = N\omega_p|d_{21}|^2/(4\varepsilon_0\hbar c)$. Eq. 41 can easily be solved for fixed $\omega$, so

$$\tilde{E}_p(z,\omega) = \tilde{E}_p(0,\omega)e^{i\kappa(\omega)z}, \tag{43}$$

where $\tilde{E}_p(0,\omega)$ stands for the Fourier transform of the probe field envelope at the entrance into the atomic medium. Finally, we obtain the desired expression for the spatio-temporal profile of the probe field envelope by taking the inverse Fourier transform:

$$E_p(z,t) = \frac{1}{2\pi}\int_{-\infty}^{\infty}\tilde{E}_p(0,\omega)e^{i(\kappa(\omega)z-\omega t)}d\omega = \frac{1}{2\pi}\int_{-\infty}^{\infty}\tilde{E}_p(0,\omega)e^{-i\left(\omega\left(t-\frac{z}{c}\right)-\alpha f(\omega)z\right)}d\omega. \tag{44}$$

By using this expression, and by knowing the temporal profile of the input probe pulse (at $z=0$), as well as the function $f(\omega)$ for both the closed (Eq. 39) and open system (Eq. 40), we numerically compute the envelope of the probe pulse as a function of the propagation distance $z$ and time $t$ for the case of the closed and open atom-lasers quantum system.

## 4. RESULTS AND DISCUSSION

In this paper, we numerically calculate the spatio-temporal profile of the probe pulse envelope during the propagation through the atomic medium, $E_p(z,t)$, under the presence of the another, control cw laser field, with the help of Eq. 44. The two distinct cases are present – the closed system, where the probe and control field couple to the energy levels of the atomic medium forming the simple ladder configuration, and the open system, where the middle level is 3-fold degenerate, and two additional levels are not coupled via any of the laser fields (Stevanović et al., 2018). To carry out the numerical calculation, we first solve OBEs for both closed and open system, by using the Fourier transform method. We concentrate on the case where the full EIT regime (maximum transparency) is established, i.e. by setting $\Delta_p = \Delta_c = 0$, and we choose the probe and control Rabi frequency by keeping in mind that the EIT condition $\Omega_p \ll \Omega_c$ has to be satisfied.

We choose to work in a system of units where $c = 1$, $\hbar = 1$, $\varepsilon_0 = 1$, $N = 1$, $\omega_p = 1$ and $d_{21} = d_{32} = 1$, which implies that $\alpha = 1/4$. Moreover, all the Rabi frequencies and detunings are assumed to be given in the units of $\gamma_0 = 1$, time is given in the units of $1/\gamma_0 = 1$, while the unit of length is also $l_0 = 1$. For the open system, the following values of the decay rates are set: $\gamma_{34} = \gamma_{35} = \gamma_{41} = \gamma_{51} = 1.0$, while $\gamma_{21}$ and $\gamma_{32}$ are considered free parameters for both the closed and open systems. Furthermore, we assume that the input pulse has the Gaussian temporal shape with the spectral half-width (one half of the pulse spectral width at $1/e$ of the field strength) $w$:

$$E_p(0,t) = E_{p0} e^{-w^2(t-t_0)^2}, \tag{45}$$

where $t_0$ is the time when the input pulse peak occurs and will be set to $t_0 = 10$ throughout the whole paper. The amplitude of the probe field strength $E_{p0}$ is connected to the amplitude of the probe Rabi frequency which is set to $\Omega_{p0} = 0.01$, so $E_{p0} = 2\hbar\Omega_{p0}/d_{21} = 0.02$. The Fourier transform of Eq. 45 gives

$$\tilde{E}_p(0,\omega) = \frac{\sqrt{\pi}\, E_{p0}}{w}\, e^{i\omega t_0}\, e^{-\left(\frac{\omega}{2w}\right)^2}, \tag{46}$$

which is also a Gaussian (with the additional phase factor $\exp(i\omega t_0)$ which does not affect the pulse profile), and which is necessary in order to solve the integral in Eq. 44. In the end, we assume that the longitudinal length (along the $z$-axis) of the sample is $L = 10$, so one can calculate the probe pulse envelope at the exit of the atomic medium as well. We thoroughly investigate how $\Omega_c$, $w$, $\gamma_{21}$, $\gamma_{32}$ and the middle-level degeneracy (differences between the closed and the open system) affect the spatio-temporal probe pulse profile due to coupling to the atomic medium and the control laser field.

The absolute value of the probe field envelope at the exit of the atomic medium ($z = L$) with respect to time is given in Fig. 2 for both the closed and open system, for several values of the control Rabi frequency $\Omega_c = 1.0, 1.5, 2.0, 5.0$ and for three different values of the spectral half-width of the pulse: $w = 0.1, 0.5, 1.0$. The following values for the remaining two decay rates are chosen: $\gamma_{21} = \gamma_{32} = 1.0$. We can clearly see that the peak value of the output pulse is notably increased as $\Omega_c$ increases, regardless of the (non-) degeneracy or the value of $w$. Since the half-width of the EIT window (one half of the spectral distance between two absorption peaks) can be estimated as $w_{\mathrm{EIT}} \approx |\Omega_c|$, it is clear that by increasing the control Rabi frequency, the transparency window broadens, which is followed by the reduction of the absorption at the center of the window (i.e. at $\Delta_p = 0$). This causes reduced absorption for the cases of larger control Rabi frequency. Moreover, it is observed that the peak heights for the open system are always smaller than for the corresponding values for the closed one. This is because the bottom value of the EIT window is determined mostly by the decay rate from the highest to the middle level – $\gamma_{32}$ for the closed system, and by $\gamma_{32} + \gamma_{34} + \gamma_{35}$ for the open system, which is of course always larger. In fact, this enables us to replace the open system with the closed system, which has the modified value of the decay rate from state $|3\rangle$ to $|2\rangle$: $\gamma_{32}^{\text{eff}} = \gamma_{32} + \gamma_{34} + \gamma_{35}$. This introduction of the so-called *effective decay rate* enables the simplification of the degenerate atomic systems of interest.

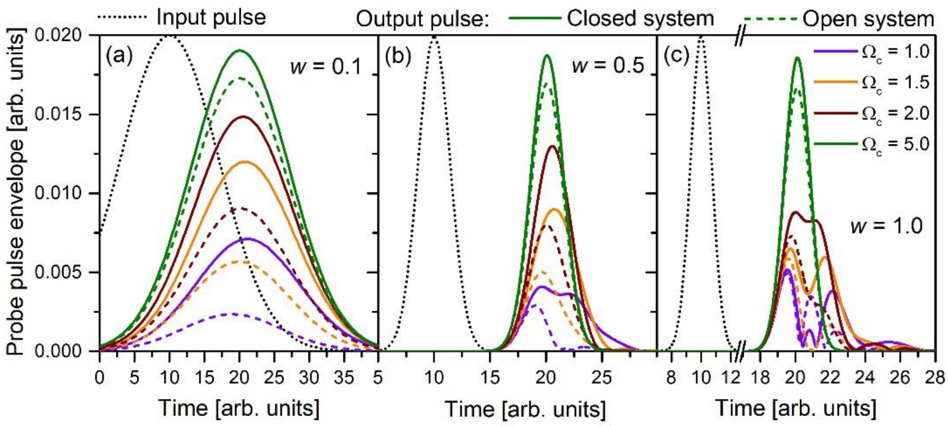


**Fig. 2** The temporal profile of the output probe pulse envelope (at $z = L$) for several values of the control Rabi frequency and for (a) $w = 0.1$, (b) $w = 0.5$ and (c) $w = 1.0$. Results for both the closed and open systems are presented. The following parameter values for decay rates are used in the computation: $\gamma_{21} = \gamma_{32} = 1.0$.

Fig. 2 also gives us information about the impact of the spectral half-width on the output pulse shape. Namely, we see that with the increase of $w$, the probe pulse has no longer the Gaussian shape for certain (smaller) values of $\Omega_c$. As we pointed out previously, the width of the EIT window is proportional to $\Omega_c$, so $w \ll \Omega_c$ for practically all the values of $\Omega_c$ in Fig. 2 (a), and all the frequency components that the pulse contains exit the medium, thus preserving the Gaussian shape of the pulse. The only absorption is the relatively small one due to the existence of the non-zero or non-negligible decay rates, particularly $\gamma_{32}$. On the other hand, in Fig. 2 (b) for $\Omega_c = 1.0$ the condition $w \ll \Omega_c$ is no longer satisfied, and those frequency components that are far apart from the carrier frequency are absorbed in the medium. As a consequence, this leads to the breakup of the pulse, which is more significant when the input spectral half-width is even larger (Fig. 2 (c)). Here, the condition $w \ll \Omega_c$ is only satisfied for $\Omega_c = 5.0$, and the Gaussian shape preservation with almost no losses is notable only for this value of the control Rabi frequency. For other values of $\Omega_c$, however, the pulse breaks up into one leading pulse and several other pulses with the variable size and shape. This can be explained as the fact that the nonlinear effects inside the medium are large enough to cause the different spectral components of the pulse to attain different group velocities (third- or higher-order effects with respect to $\omega$). This behavior is the same for both the closed and open systems, except that the pulse breakup is not that significant for the open system due to larger absorption at the center of the transparency window.

In Fig. 3, the spatio-temporal profile of the absolute value of the probe pulse is given for the closed and the open quantum system, and for three values of the spectral half-width: $w = 0.2, 1.0, 5.0$. The value of the control Rabi frequency is set to $\Omega_c = 2.0$, while again $\gamma_{21} = \gamma_{32} = 1.0$. We can see that, for the closed system and for the smaller spectral half-width, as in Fig. 3 (a), the pulse propagates through the medium with certain losses (due to large $\gamma_{32}$), but without changing the Gaussian shape of the pulse. As $w$ increases, the pulse cannot pass through the EIT window as a whole and some frequency components remain absorbed inside the medium. This is particularly visible in Fig. 3 (c), with the initial pulse being split into one leading pulse and several following smaller pulses, thus significantly deforming the initial structure of the pulse. By looking at Fig. 3 (d–f) which depict the pulse propagation through the degenerate atomic system, it can again be observed that the absorption of the pulse is more significant than in the case of the closed system, although the same conclusions can be made for the open system as far as the breakup of the pulse is concerned.

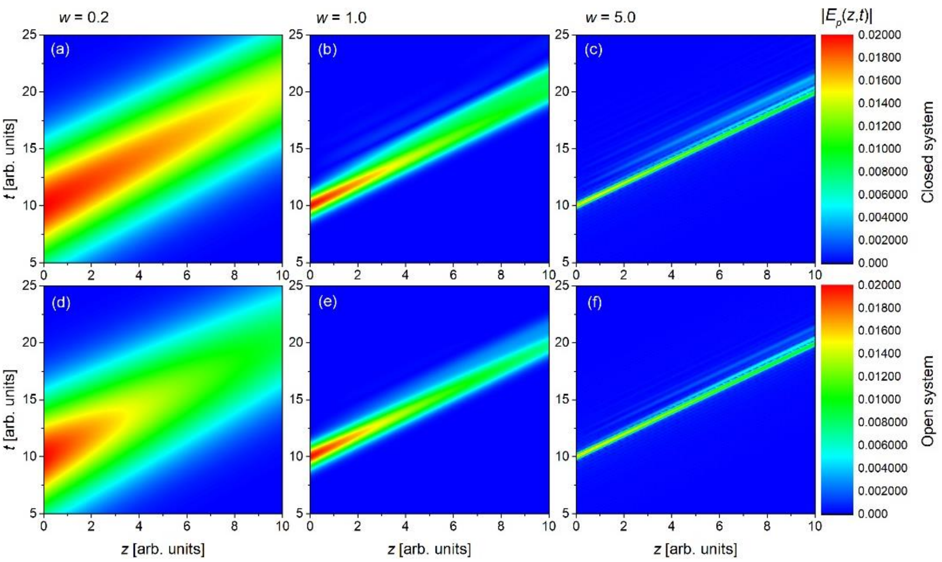


**Fig. 3** The absolute value of the probe pulse envelope with respect to distance and time, for the (a–c) closed system and (d–f) open system. The chosen values of the spectral half-width are (a, d) $w = 0.2$, (b, e) $w = 1.0$ and (c, f) $w = 5.0$, while $\Omega_c = 2.0$ and $\gamma_{21} = \gamma_{32} = 1.0$.

We now concentrate on the influence of the decay rates $\gamma_{21}$ and $\gamma_{32}$ on the output probe pulse. The absolute value of the probe field envelope with respect to time is given in Fig. 4 for closed and open systems, for several values of $\gamma_{21}$ and $\gamma_{32}$. The control Rabi frequency is $\Omega_c = 2.0$ and the spectral half-width is $w = 0.8$. In Fig. 4 (a), the value of

$\gamma_{21}$ is fixed to $\gamma_{21} = 1.0$, while the other decay coefficient takes the values: $\gamma_{32} = 0.5, 1.0, 1.5, 2.0$. It is already mentioned that the value of $\gamma_{32}$ ($\gamma_{32} + \gamma_{34} + \gamma_{35}$) is mainly responsible for the value of the bottom of the EIT window for the closed (open) system. Therefore, the increase of these decay rates (here, we only increase $\gamma_{32}$ for the open system, keeping $\gamma_{34}$ and $\gamma_{35}$ constant) leads to the increase of the absorption at the bottom of the EIT window, and further to the decrease of the pulse peak height at the exit of the medium. Of course, this decrease is more notable for the open system due to the larger "effective" decay rate from the highest to the middle level(s). In all cases, a significant decrease in the peak height is observed. This is due to the fact that the values of the decay rates and $\Omega_c$ are of the same order of magnitude. It can be shown that, in order to obtain even more efficient transmission, one has to increase the value of the control Rabi frequency at least to the one order of magnitude higher value than those of $\gamma_{21}$ and $\gamma_{32}$. Fortunately, this is feasible for a huge number of atom-lasers systems used in the EIT-related experiments.

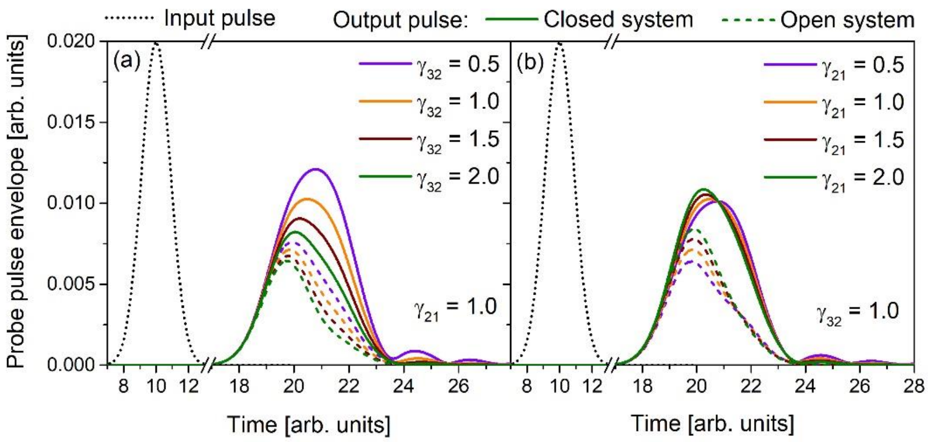


**Fig. 4** The temporal profile of the output probe pulse envelope (a) for $\gamma_{21} = 1.0$ and several values of $\gamma_{32}$ and (b) for $\gamma_{32} = 1.0$ and several values of $\gamma_{21}$. Results for both the closed and open systems are presented. The following parameter values are used: $\Omega_c = 2.0$ and $w = 0.8$.

In Fig. 4 (b), the value of $\gamma_{32}$ is fixed to $\gamma_{32} = 1.0$, while $\gamma_{21}$ is allowed to change: $\gamma_{21} = 0.5, 1.0, 1.5, 2.0$. All the other parameters have the same values as in Fig. 4 (a). We notice that there is no significant change in the output pulse shape with respect to $\gamma_{21}$ – even though there are some slight changes in the pulse shape, the impact of the value of $\gamma_{21}$ on the transmission of the pulse is clearly negligible. More precisely, even though the leading pulse has a slightly larger peak value for a certain value of $\gamma_{32}$ (for instance, for $\gamma_{32} = 2.0$ compared to $\gamma_{32} = 0.5$), the peak values of the pulses which follow the leading one will be comparably smaller. On the basis of this discussion, as well as of the one from the previous text, we can conclude that the influence of the decay rate $\gamma_{32}$ on the probe pulse propagation is far more expressed than the one of the coefficient $\gamma_{21}$.

Until now, we focused on the temporal shape of the probe pulse with respect to several parameters. However, it is important to investigate how specific quantities, closely related to the pulse, depend on the same parameters. To do this, we first define the pulse energy at the entrance and at the exit of the atomic medium, $W_{\text{in}}$ and $W_{\text{out}}$, respectively, mean value $\langle t^n \rangle$ and standard deviation for the intensity of the output pulse $\sigma_{\text{out}}$ (proportional to the temporal width of the output pulse) using the following formulas (Nielsen et al., 2007):

$$W_{\text{in}} = \int_{-\infty}^{\infty} \left| E_p\,(0,t) \right|^2 dt, \tag{47}$$

$$W_{\text{out}} = \int_{-\infty}^{\infty} \left| E_p\,(L,t) \right|^2 dt, \tag{48}$$

$$\langle t^n \rangle = \frac{1}{W_{\text{out}}} \int_{-\infty}^{\infty} t^n \left| E_p\,(L,t) \right|^2 dt\,,\; n \;=\; 1,2, \tag{49}$$

$$\sigma_{\text{out}} = \sqrt{\langle t^2 \rangle \,-\, \langle t \rangle^2}. \tag{50}$$

We are interested in the value of the group index $n_g \;=\; c/v_g$, which is obtained with the help of the following formula for the group velocity of the pulse:

$$v_g \;=\; \frac{L}{\langle t \rangle - t_0}. \tag{51}$$

The other parameter of interest is the relative temporal width of the output pulse, $\sigma_{\text{out}}/\sigma$, where $\sigma \;=\; 1/(2w)$ is the standard deviation for the intensity of the input pulse. Since also $w_{\text{out}} \;=\; 1/(2\sigma_{\text{out}})$ we have $\sigma_{\text{out}}/\sigma \;=\; w/w_{\text{out}}$, so the relative temporal width instantly gives the relative spectral width of the output pulse. In the end, we define the transmission coefficient as $T \;=\; W_{\text{out}}/W_{\text{in}}$. We study the behavior of $n_g$, $\sigma_{\text{out}}/\sigma$ and $T$ with respect to both the control Rabi frequency $\Omega_c$ and the input pulse spectral half-width $w$.

In Fig. 5, all the relevant parameters (group index, relative temporal pulse width, and transmission coefficient) are given with respect to $\Omega_c$ (for fixed $w \;=\; 0.5$) and $w$ (for fixed $\Omega_c = 2.0$), for the closed as well as for the open system. All the graphs are obtained by taking $\gamma_{21} = \gamma_{32} = 1.0$. By looking at Fig. 5 (a) for both the closed and open system, it can be seen that the value of $n_g$ does not change monotonically with the increase of $\Omega_c$ – at first, as the control Rabi frequency increases, $n_g$ decreases, which is followed by the increase of $n_g$ with the further increase of $\Omega_c$, after which the group index asymptotically tends to unity (horizontal asymptote described by the black dashed line). Therefore, in both cases, the minimum of the group index occurs, and the values of these two minima are smaller than unity for this particular set of parameters. However, the range of values of the control Rabi frequency $\delta\Omega_c$ for which $n_g < 1$ is larger for the case of the open system. This means that the fast light region is accessible with a larger range of $\Omega_c$ for the open system ($\Omega_c \in (0.55, 1.63)$, $\delta\Omega_c \approx 1.08$) compared to the closed one ($\Omega_c \in (0.40, 0.71)$, $\delta\Omega_c \approx 0.31$). Outside of these regions, the regime of slow light is achieved. The similar conclusion can be made by looking at Fig. 5 (d), where the dependence of $n_g$ on $w$ is studied – for this particular choice of parameters, one can achieve the fast light regime only for a small region of initial pulse half-widths for the open system, but not for the closed one. In both cases, as in Fig. 5 (a), there is a horizontal asymptote which is equal to unity, and the group velocity of light is equal to the vacuum speed of light for large values of both $\Omega_c$ and $w$.

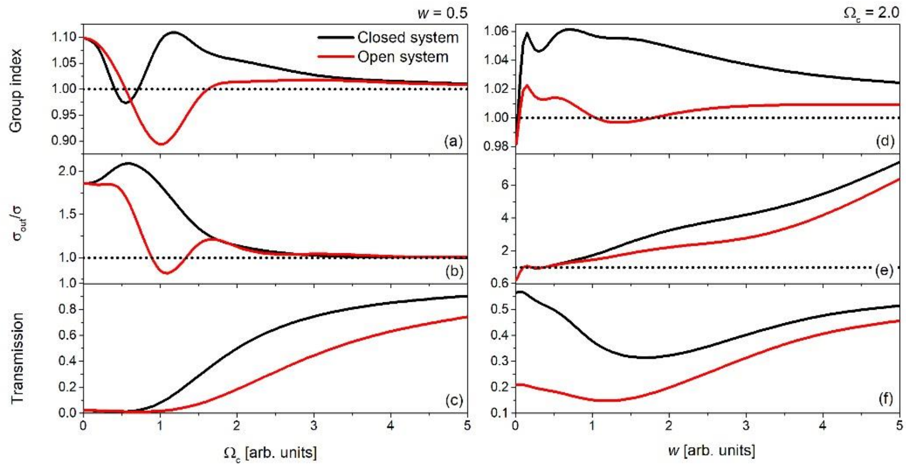


**Fig. 5** The dependence of the (a, d) group index, (b, e) relative temporal pulse width and (c, f) transmission coefficient on the (a–c) control field Rabi frequency (with $w = 0.5$) and (d–f) spectral half-width of the input pulse (with $\Omega_c = 2.0$). The results are obtained by taking $\gamma_{21} = \gamma_{32} = 1.0$.

As far as the relative temporal output pulse width is concerned, we can see its dependence on $\Omega_c$ in Fig. 5 (b) and on $w$ in Fig. 5 (e). It is observed that $\sigma_{\text{out}}/\sigma$ is large for smaller values of $\Omega_c$, while for large values of the control Rabi frequency it tends to unity (black dotted line). This is reasonable since the EIT window is very narrow when $\Omega_c$ is small (to be more precise, there would be no EIT window at all due to the violation of the EIT condition $\Omega_{\text{p}} \ll \Omega_c$, but one absorption peak at $\Delta_p = 0$, and almost all the frequency components will be absorbed). Therefore, many frequency components are absorbed by the atomic medium, so the output pulse is narrowed in frequency, i.e. temporally broadened. The same explanation can be used for the behavior of $\sigma_{\text{out}}/\sigma$ in Fig. 5 (e) for large $w$ – the output pulse is spectrally narrowed due to the absorption of many frequency components of the pulse, which leads to an increase in the duration of the pulse. On the other hand, when $\Omega_c$ is large enough (Fig. 5 (b)), $w \ll \Omega_c$ is satisfied, so no frequency components get absorbed and the pulse propagates without changing its shape and width. The same condition is satisfied for small values of $w$ in Fig. 5 (e), which is why there exists a region where the relative pulse width is unity as well. In addition, we note the existence of the minimum in Fig. 5 (b) for the open system, with the value $\sigma_{\text{out}}/\sigma < 1$. Therefore, there is a range of values of the control Rabi frequency for which the temporal narrowing of the pulse can be achieved ($\Omega_c \in (0.88, 1.34)$), and it is connected to the fast light regime (see Fig. 5 (a)). This is, however, possible only for the open quantum system.

In the end, let us focus on the dependence of the transmission coefficient on $\Omega_c$ (Fig. 5 (c)) and $w$ (Fig. 5 (f)). As one should expect, since no EIT has been achieved for the small values of the control Rabi frequency, the transmission is almost equal to zero. By the further increase in $\Omega_c$, when the EIT window is established, the transmission coefficient increases. Since the width of the transparency window is linearly dependent on $\Omega_c$, almost all the pulse exits the medium when the value of this width is large enough. Since the bottom of the EIT window is determined by the value of $\gamma_{32}$ and this value is of the same order of magnitude as $\Omega_c$, absorption losses cannot be neglected. Only with the further increase of $\Omega_c$ ($\Omega_c > 5.0$) one can reduce losses (the value of the bottom of the EIT window decreases) causing the transmission coefficient to be nearly equal to unity. Moreover, this value of $T \approx 1$ is achieved "faster" for the closed system – for the open system, one has to increase $\Omega_c$ even more compared to the closed system in order to obtain the maximum transmission. As far as the dependence of $T$ on the input spectral half-width is concerned, it is clear that the transmission is maximal when $w$ is small and all the pulse transmits through the medium. As $w$ increases, however, the transmission decreases due to the absorption of various spectral components and saturates for large values of $w$. This can be explained in the following way: no matter how large $w$ is chosen, several spectral components of the pulse near the carrier frequency will always be transmitted through the medium, and there will be no change of the energy of the output pulse.

## 5. Conclusion

In this paper, we investigated the propagation of the weak probe pulse through the atomic medium in the presence of the additional, strong control cw laser field. The two lasers and the medium couple to each other and form the ladder coupling scheme. We focused on the two cases: the closed system, which represents the standard 3-level ladder scheme, and the open system, where the middle level is 3-fold degenerate. In order to calculate the spatio-temporal profile of the pulse envelope, we used the formalism of Maxwell-Bloch equations, with the help of the Fourier transform method. We examined the influence of the middle-level degeneracy on the propagation of the probe pulse and concluded that one can replace the open system with the appropriate closed system with the effective value of the decay rate from the highest to the middle level. Since the decay rates from the highest to the sublevels of the middle level of the open system add up, the pulse gets absorbed more quickly if the medium is the system with degenerate levels compared to the non-degenerate case. Moreover, we studied the impact of the control field Rabi frequency and the spectral half-width of the input pulse, as well as the decay rates, on the shape of the output pulse. We found that the ratio between the control Rabi frequency and spectral half-width is important since it determines what spectral components of the pulse can be transmitted through the transparency window. As a consequence, the output pulse can either retain the initial Gaussian temporal shape if the spectral half-width is much smaller than $\Omega_c$, or can break up into one leading and several smaller pulses which propagate with different group velocities for the case when $w$ is similar or larger than $\Omega_c$. We also found that among the two decay rates we focused our attention, $\gamma_{32}$ has a larger impact on the output pulse profile compared to $\gamma_{21}$, since it is this value that is responsible for the value of the bottom of the transparency window, determining the absorption of the pulse. In the end, we calculated the values of the group index, relative pulse width and transmission coefficient with respect to both $\Omega_c$ and $w$, for both the closed and open system. It is observed that both the control Rabi frequency and spectral half-width strongly affect these values. For instance, by changing these parameters, one can reduce or increase the group velocity of light and switch between the slow- or fast-light regime. There is a range of parameters for which the realization of fast light is possible, while the other parameter values correspond to slow light, and this range is larger for the open system. In fact, fast light in the closed system might not occur at all regardless of the values of the considered parameters, even if there exists a region where fast light in the open system is achievable. We believe that this research could help the study of these types of quantum systems, which is of great interest in order to further develop the fields of quantum optics, optical telecommunications and quantum information processing.

## REFERENCES

Badger, S.D., Hughes, I.G., Adams, C.S., 2001. J. Phys. B: At. Mol. Opt. Phys., 34, L749–L756, doi:10.1088/0953-4075/34/22/107

Boller, K.-J., Imamoğlu, A., Harris, S. E., 1991. Phys. Rev. Lett., 66, 2593–2596, doi:10.1103/PhysRevLett.66.2593

Boyd, R. W., 2007. Nonlinear Optics, 3rd Edition, Academic Press.

Boyd, R. W., Gauthier, D. J., 2009. Science, 326, 1074–1077, doi:10.1126/science.1170885

Boyd, R. W., Narum, P., 2007. J. Mod. Opt., 54, 2403–2411, doi:10.1080/09500340701639649

Budker, D., Kimball, D.F., Rochester, S.M., Yashchuk, V.V., 1999. Phys. Rev. Lett., 83, 1767–1770, doi:10.1103/PhysRevLett.83.1767

Fleischhauer, M., Imamoğlu, A., Marangos, J. P., 2005. Rev. Mod. Phys., 77, 633–673, doi:10.1103/RevModPhys.77.633

Guan, P.-C., Yu, I. A., 2000. Phys. Rev. A, 61, 053805:1–6, doi:10.1103/PhysRevA.76.033817

Harris, S. E., Field, J. E., Kasapi, A., 1992. Phys. Rev. A, 46, R29–32, doi:10.1103/PhysRevA.46.R29

Hau, L. V., Harris, S. E., Dutton, Z., Behroozi, C. H., 1999. Nature, 397, 594–598, doi:10.1038/17561

Kash, M. M., Sautenkov, V. A., Zibrov, A. S., Hollberg, L., Welch, G. R., Lukin, M. D., Rostovtsev, Y., Fry, E. S., Scully, M. O., 1999. Phys. Rev. Lett., 82, 5229–5232, doi:10.1103/PhysRevLett.82.5229

Li, T., Lu, M.-J., Weinstein, D., 2011. Phys. Rev. A, 84, 023801:1–6, doi:10.1103/PhysRevA.84.023801

Li, Y.-q., Xiao, M., 1995. Phys. Rev. A, 51, R2703–R2706, doi:10.1103/physreva.51.r2703

Lukin, M. D., 2003. Rev. Mod. Phys., 75, 457–472, doi:10.1103/RevModPhys.75.457

Marangos, J. P., 1998. J. Mod. Opt., 45, 471–503, doi: 10.1080/09500349808231909

Menzel, R., 2007. Photonics, Linear and Nonlinear Interactions of Laser Light and Matter, 2nd Edition, Springer, Berlin.

Moon, H.S., Noh, H.-R., 2013. Opt. Express, 21, 7447–7455, doi:10.1364/OE.21.007447

Nielsen, P. K., Thyrrestrup, H., Mork, J., Tromborg, B., 2007. Opt. Express, 15, 6396–6408, doi:10.1364/OE.15.006396

Noh, H.-R., Moon, H. S., 2009. Phys. Rev. A, 80, 022509:1–5, doi:10.1103/PhysRevA.80.022509

Noh, H.-R., Moon, H. S., 2012. Phys. Rev. A, 85, 033817:1–5, doi:10.1103/PhysRevA.85.033817

Pavlović, V., Stevanović, Lj., 2016. Superlatt. Microstruct., 92, 10–23, doi:10.1016/j.spmi.2016.02.003

Pavlović, V., Šušnjar, M., Petrović, K., Stevanović, Lj., 2018. Opt. Mater., 78, 191–200, doi:10.1016/j.optmat.2018.01.043

Reshetov, V. A., Meleshko, I. V., 2014. Laser Phys., 24, 094011:1–7, doi:10.1088/1054-660X/24/9/094011

Schmidt, H., Ram, R. J., 2000. Appl. Phys. Lett., 76, 3173–3175, doi:10.1063/1.126620

Scully, M. O., Zubairy, M.S., 1997. Quantum optics, Cambridge University Press, Cambridge.

Stevanović, Lj., Filipović, N., Pavlović, V., 2018. Opt. Quant. Electron., 50, 287:1–12, doi:10.1007/s11082-018-1554-5

Vitali, D., Fortunato, M., Tombesi, P., 2000. Phys. Rev. Lett., 85, 445–448, doi:10.1103/PhysRevLett.85.445

Zhang, S., Zhou, S., Loy, M. M. T., Wong, G. K. L., Du, S., 2011. Opt. Lett., 36, 4530–4532, doi:10.1364/OL.36.004530

# PROSTIRANJE SPORE I BRZE SVETLOSTI KROZ ATOMSKE SREDINE SA DEGENERISANIM NIVOIMA U LESTVIČASTOJ KONFIGURACIJI

*Proučava se prostiranje sondirajućeg pulsa slabog intenziteta kroz atomsku sredinu, u prisustvu kontrolnog laserskog polja jakog intenziteta, i u uslovima ostvarene elektromagnetno indukovane transparentnosti (EIT). Pomenuta polja su spregnuta sa sredinom i formiraju lestvičastu konfiguraciju sa tri nivoa. Razmatraju se dva slučaja: nedegenerisani, zatvoren sistem, kao i otvoren sistem u kome je središnji energijski nivo trostruko degenerisan, a dodatni nivoi sprežu se sa ostalim nivoima samo preko spontane emisije. Prostorno-vremenski profil envelope sondirajućeg pulsa dobijen je korišćenjem formalizma Maksvel-Blohovih jednačina, uz pomoć metoda Furijeove transformacije. Proučavan je uticaj Rabijeve frekvencije kontrolnog polja, spektralne poluširine inicijalnog pulsa, kao i koeficijenata raspada na prostiranje sondirajućeg pulsa. Računato je i nekoliko važnih parametara koji se tiču sondirajućeg pulsa. Pokazano je da je moguće kontrolisati grupnu brzinu svetlosti tako da se, promenom kontrolne Rabijeve frekvencije i spektralne poluširine pulsa, može vršiti prelazak iz spore u brzu svetlost i obrnuto. Takođe, razmatrana je i mogućnost zamene otvorenog sa efektivnim zatvorenim sistemom.*

Ključne reči: *Elektromagnetno indukovana transparentnost, spora svetlost, brza svetlost, degeneracija energijskih nivoa, zatvoren sistem, otvoren sistem*